J|A|C|S
ARTICLES
Published on Web 02/27/2003

Covalent Sidewall Functionalization of Single Wall Carbon Nanotubes

Rajesh K. Saini, Ivana W. Chiang, Haiqing Peng, R. E. Smalley, W. E. Billups,* Robert H. Hauge, and John L. Margrave

Contribution from the Center for Nanoscale Science and Technology, Rice Quantum Institute, Department of Chemistry, Rice University, Houston, Texas 77005

Received September 10, 2002; E-mail: billups@rice.edu

Abstract: Alkyllithium reagents may be used to attach alkyl groups to the sidewalls of fluoro nanotubes. Thermal gravimetric analysis combined with UV−vis−Nir spectroscopy has been used to provide a quantitative measure of the degree of functionalization. SWNTs prepared using the HiPco process exhibit a higher degree of alkylation than SWNTs from the laser-oven method, indicating that the smaller diameter fluoro tubes are alkylated more readily. The spectral signature of the pristine SWNTs can be regenerated when the alkylated SWNTs are heated in Ar at 500 °C, demonstrating that dealkylation occurs at this temperature. TGA−MS analysis using a sample of *n*-butylated h-SWNTs showed that 1-butene and *n*-butane are formed during thermolysis.

Introduction

Nanometer scale structures have become the focus of considerable interest because they represent ideal systems for testing fundamental ideas about the roles of dimensionality and confinement in materials, and represent potential building blocks for nanostructured materials, composites, and novel electronic devices of greatly reduced size. Among the wide range of nanometer scale structures prepared to date, carbon nanotubes and, in particular, single-wall carbon nanotubes (SWNTs) stand out as unique materials for fundamental research and emerging applications.[1−6] For example, carbon nanotubes are the stiffest known materials,[7] exhibit novel electronic properties that bridge the bulk and molecular states,[8−10] and represent a flexible starting point for preparing new nanomaterials.[5,11−13]

In some cases, chemical modification will be required if these materials are to reach their full potential. However, this area of research presents enormous challenges and results have been slow to emerge.[14−18] Haddon[19] has reported that nanotubes may be solvated by reacting octadecylamines with the carboxylic acid groups that are bound to the ends of the tubes. Addition of dichlorocarbene to the sidewalls of tubes was also reported. Lieber[20] and co-workers demonstrated that carboxyl acid groups attached to the ends of the nanotubes function as AFM tips. Mickelson demonstrated a high degree of sidewall derivatization by fluorination.[21,22] The fluorinated materials can be further functionalized by displacing fluoride with alkyl groups.

Two methods now dominate the production of SWNTs. The older method involves laser vaporization of a metal-doped target in a hot oven.[13] More recently, a new gas phase process that operates by catalytically disproportionating high-pressure CO using an iron catalyst has been developed (HiPco process).[3] This process leads to raw material that can be purified to yield highly purified SWNTs. Cleaning procedures have been developed that remove the metal and nonnanotube carbon.[13,27,28]

(1) Iijima, S. *Nature* **1991**, *354*, 56.
(2) Iijima, S.; Ichihashi, T. *Nature* **1993**, *363*, 603.
(3) Thess, A.; Lee, R.; Nikolaev, P.; Dai, H.; Petit, P.; Robert, J.; Xu, C.; Lee, Y.; Kim, S.; Colbert, D.; Smalley, R. E. *Science* **1996**, *273*, 483.
(4) Bethune, D. S.; Kaing, C. H.; de Vries, M. S.; Gormand, G.; Savoy, R.; Vazquez, J.; Beyers, R. *Nature* **1993**, *363*, 605.
(5) Rinzler, A. G.; Hafner, J. H.; Nikolaev, P.; Lou, L.; Kim, S. G.; Tomanek, D.; Nordlander, P.; Colbert, D. T.; Smalley, R. E. *Science* **1995**, *269*, 1550.
(6) Ajayan, P. M.; Lambert, J. M.; Bernier, P.; Barbedette, L.; Colliex, C.; Planeix, J. M. *Chem. Phys. Lett.* **1993**, *215*, 509.
(7) Lieber, C. M.; Morales, A. M.; Sheehan, P. E.; Wong, E. W.; Yang, P. In *Chemistry on the Nanometer Scale*; Robert A. Welch Foundation 40th conference on chemical research: Houston, Texas, 1997.
(8) Dai, H.; Wong, E. W.; Lieber, C. M. *Science* **1996**, *272*, 523.
(9) Tans, S. J.; Devoret, M. H.; Groeneveld, R. J.; Dekker, C. *Nature* **1998**, *394*, 761.
(10) Bockrath, M.; Cobden, D. H.; McEuen, P. L.; Chopra, N. G.; Zettl, A.; Thess, A.; Smalley, R. E. *Science* **1997**, *275*, 1922.
(11) Dai, H.; Wong, E. W.; Lu, Y. Z.; Fan, S.; Lieber, C. M. *Nature* **1995**, *375*, 769.
(12) Wong, E. W.; Maynor, B. W.; Burns, L. D.; Lieber, C. M. *Chem. Mater.* **1996**, *8*, 2041.
(13) Rinzler, A.; Liu, J.; Dai, H.; Nikolaev, P.; Huffman, C.; Rodriguez-Macias, F.; Boul, P.; Lu, A.; Heymann, D.; Colbert, D. T.; Lee, R. S.; Fischer, J.; Rao, A.; Eklund, P. C.; Smalley, R. E. *Appl. Phys. A* **1998**, *67*, 29.
(14) Dujardin, E.; Ebbesen, T. W.; Krishnan, A.; Treacy, M. M. *Adv. Mater.* **1998**, *10*, 1472.
(15) Garg, A.; Sinnott, S. B. *Chem. Phys. Lett.* **1998**, *295*, 273.
(16) Mawhinney, D. B.; Naumenko, V.; Kuznetsova, A. Y.; Liu, J.; Smalley, R. E. *J. Am. Chem. Soc* **2000**, *122*, 2383.
(17) Riggs, J. E.; Guo, Z.; Carroll, D. L.; Sun, Y.-P. *J. Am. Chem. Soc* **2000**, *122*, 5879.
(18) Jaffe, R. L. *Proc.-Electrochem. Soc.* **1999**, *99*, 153.
(19) Hamon, M. A.; Chen, J.; Hu, H.; Chen, Y. S.; Itkis, M. E.; Rao, A. M.; Eklund, P. C.; Haddon, R. C. *Adv. Mater.* **1999**, *11*, 834.
(20) Wong, S. S.; Joselevich, E.; Woolley, A. T.; Cheung, L.; Lieber, C. M. *Nature* **1998**, *394*, 52.
(21) Mickelson, E. T.; Huffman, C. B.; Rinzler, A. G.; Smalley, R. E.; Hauge, R. H.; Margrave, J. L. *Chem. Phys. Lett.* **1998**, *296*, 188.
(22) Kelly, K. F.; Chiang, I. W.; Mickelson, E. T.; Hauge, R. H.; Margrave, J. L.; Wang, X.; Scuseria, G. E.; Radloff, C.; Halas, N. J. *Chem. Phys. Lett.* **1999**, *313*, 445.
(23) Boul, P. J.; Liu, J.; Mickelson, E. T.; Huffman, C. B.; Ericson, L. M.; Chiang, I. W.; Smith, K. A.; Colbert, D. T.; Hauge, R. H.; Margrave, J. L.; Smalley, R. E. *Chem. Phys. Lett.* **1999**, *310*, 367.
(24) Dai, H.; Rinzler, A. G.; Nikolaev, P.; Thess, A.; Colbert, D. T.; Smalley, R. E. *Chem. Phys. Lett.* **1996**, *260*, 471.

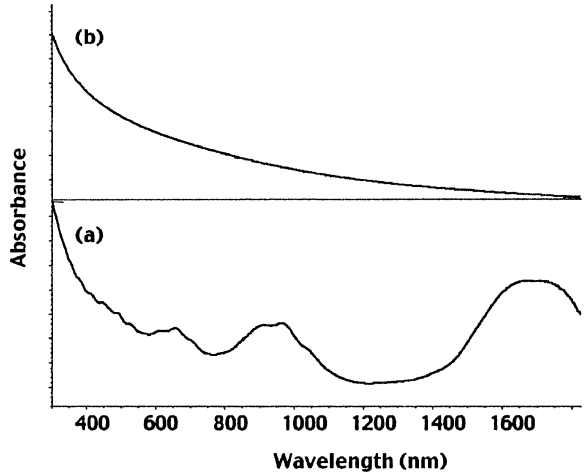

Figure 1. UV−vis−Nir spectra of pristine and hexylated l-SWNTs recorded in Triton-X/D_2O solution. (a) Pristine l-SWNTs; (b) *n*-hexylated l-SWNTs.

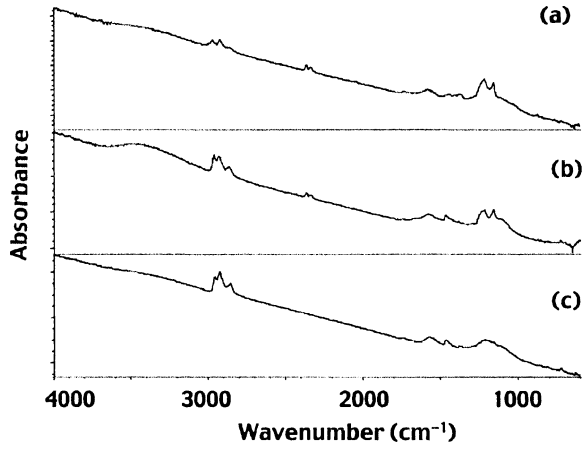

Figure 2. FTIR spectra taken with ATR accessory of alkylated l-SWNTs. (a) methylated l-SWNTs; (b) *n*-butylated l-SWNTs; (c) *n*-hexylated l-SWNTs.

In this paper, we present an up-to-date account of recent results on the use of fluorinated nanotubes produced by both the laser oven method (l-SWNTs) and the HiPco process (h-SWNTs) as intermediates for sidewall alkylation.

Experimental Section

General. Single wall carbon nanotubes produced by the laser oven method (l-SWNTs) and the HiPco process (h-SWNTs) were obtained from Rice University.[24,25,26] The SWNTs were purified as described previously.[13,27,28] SWNTs with residual metal less than 0.1 atomic percent and impurity carbon less than 1 wt. percent were obtained after purification. Thermogravimetric (TGA) data were obtained using a model 2960 TA instrument. IR, mass spectra and TGA experiments were carried out with SWNTs in the form of buckypaper. Samples for

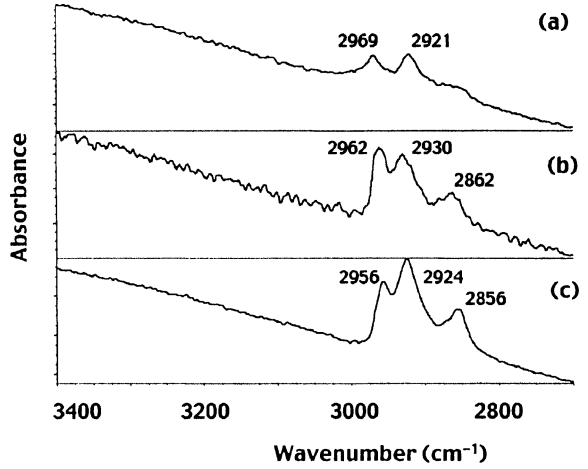

Figure 3. FTIR spectra taken with ATR accessory of alkylated l-SWNTs. The numbers in the spectra denote the peak location. (a) methylated l-SWNTs; (b) *n*-butylated l-SWNTs; (c) *n*-hexylated l-SWNTs.

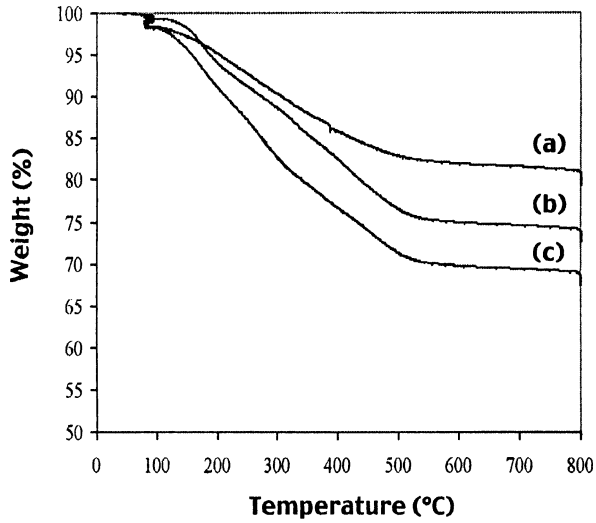

Figure 4. TGA weight loss vs temperature plot of degassed alkylated l-SWNTs. Experiments were carried out in argon. Samples were degassed at 80 °C and then heated 10 °C/min to 800 °C and held there for 30 min. (a) methylated l-SWNTs; (b) *n*-butylated l-SWNTs; (c) *n*-hexylated l-SWNTs.

UV−vis−Nir spectroscopy were prepared by sonicating the SWNTs for ~10 min in 0.15 wt % Triton-X D_2O solution with a cup sonicator. UV−vis−Nir spectra were obtained with a Shimadzu UV-3101 PC spectrometer. FTIR spectra were obtained using a Nicolet spectrometer with the ATR accessory. TGA-MS analyses were carried using a Q 500 TA instrument.

Fluorination. Fluorination reactions were carried out using the procedure described previously.[21] In this case, HF (2.0 sccm) was introduced as a catalyst into the F_2/He (2.0 sccm, 20 sccm respectively) mixture during fluorination. Laser-oven SWNTs were fluorinated at 250 °C and HiPco nanotubes at 150 °C. It has been found empirically that the smaller diameter HiPco nanotubes fluorinate to the nominal C_2F stoiciometry at a lower temperature than l-oven SWNTs.

General Procedure for Alkylation. 10 mg of the fluorinated nanotubes (HiPco, C_2F stoiciometry) were added to a flame dried 100 mL three-necked round-bottomed flask under an atmosphere of argon (baloon). Dry hexane (5 mL) was then added and the contents were sonicated for 5 min (VWR scientific model 50 HT). The resulting suspension was cooled to − 40 °C in an ice−acetone bath. An excess of the alkyllithium in hexane or ether (0.02 mol) was then added dropwise to the resulting suspension via a syringe. The solution was stirred for 1 h at −40 °C, warmed to room temperature, and stirred

(25) Bronikowski, M. J.; Willis, P. A.; Colbert, D. T.; Smith, K. A.; Smalley, R. E. *J. Vac. Sci. Technol. A*, **2001**, *19(4)*, 1801.
(26) Hafner, J. H.; Bronikowski, M. J.; Azamian, B. R.; Nikolaev, P.; Rinzler, A. G.; Colbert, D. T.; Smith, K. A.; Smalley, R. E. *Chem. Phys. Lett.* **1998**, *296*, 195.
(27) Chiang, I. W.; Brinson, B. E.; Smalley, R. E.; Margrave, J. L.; Hauge, R. H. *J. Phys. Chem. B* **2001**, *105*, 1157.
(28) Chiang, I. W.; Brinson, B. E.; Huang, A. Y.; Willis, P. A.; Bronikowski, M. J.; Margrave, J. L.; Smalley, R. E.; Hauge, R. H. *J. Phys. Chem. B* **2001**, *105*, 8297.
(29) If *n*-hexane, formed by hydrolysis of the *n*-hexyllithium during workup, was adsorbed onto the SWNTs it would have been expected to evaporate at a much lower temperature as the boiling point of *n*-hexane is 69 °C. A control experiment in which *n*-hexane was added to virgin tubes and submitted for TGA analysis after being heated to 80 °C for 12 h under vacuum showed no evolution of *n*-hexane.

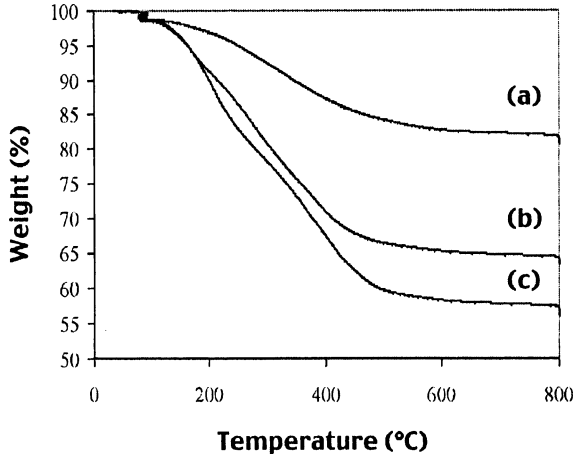

Figure 5. TGA weight loss vs temperature plot of degassed alkylated h-SWNTs. Experiments were carried out in argon. Samples were degassed at 80 °C and then heated 10 °C/min to 800 °C and held there for 30 min. (a) methylated h-SWNTs; (b) *n*-butylated h-SWNTs; (c) *n*-hexylated h-SWNTs.

Table 1. Carbon/Alkyl Group Ratios Calculated from TGA Weight Loss Data for (a) Methyl SWNTs; (b) *n*-butyl SWNTs; (c) *n*-Hexyl SWNTs for HiPco and Laser-Oven-Grown Nanotubes[a]

	HiPco	laser-oven-grown
(a)	6.6	6.0
(b)	9.4	14.7
(c)	10.0	18.0

[a] Several runs gave reproducible results when the same batch of fluorinated material was used.

overnight. The solution was then cooled in an ice bath and the unreacted lithium reagent quenched by the slow addition of ethanol. Water (50 mL) was added to dissolve the resulting salts. The nanotubes were then filtered using PTFE filter paper (0.45 μm) and washed with water. The nanotubes were then suspended in 3N HCl, sonicated for 15 min, filtered, and washed with water. This procedure was repeated using hot ethanol. The final product was dried overnight in vacuo at 80 °C to afford the alkylated nanotubes.

Methylated nanotube, yield 6.2 mg.

Butylated nanotubes, yield 8.0 mg.

Hexylated nanotubes, yield 9.0 mg.

The degree of functionalization from the same batch of fluorinated material gave nearly identical results. The extent of alkylation depends on the degree of fluorination.

Result and Discussion

UV−vis−Nir serves as an excellent monitor for sidewall perturbation of nanotubes. This may be attributed to rehybridization at carbon (sp^2 to sp^3) because the π electrons in the highest occupied molecular orbitals (HOMOs) that are used to form new bonds are no longer available and the van Hove transitions vanish. The UV−vis−Nir spectra of pristine and hexylated l-SWNTs are displayed in Figure 1. The absence of electronic transitions for the hexylated SWNTs supports the assumption that sidewall functionalization by *n*-hexyl groups has occurred.

Infrared spectra of alkylated l-SWNTs are shown in Figure 2. The alkyl substituents exhibit typical C−H stretching absorptions at 2850−2970 cm^{-1}. As expected, the relative intensity of the C−H stretching absorption is higher when the SWNTs are functionalized by *n*-hexyl groups (Figure 3). Each material exhibits a peak (Figure 2) at ~1578 cm^{-1} that can be

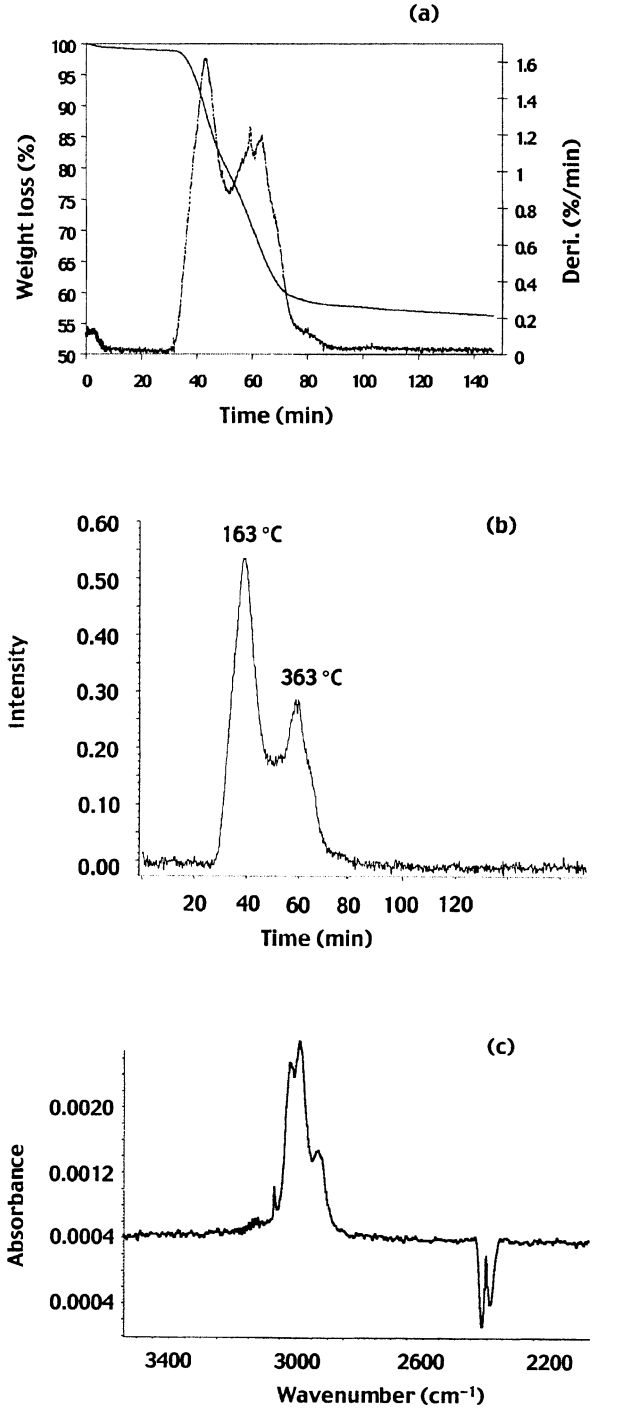

Figure 6. TGA-FTIR spectra of hexylated h-SWNTs. (a) TGA weight loss vs time and derivative of weight loss vs time plots. Experiments were carried out in argon. Samples were degassed at 80 °C, then heated 10 °C/min to 800 °C and held there for 30 min. (b) Chemigram of hexyl groups evolving from 0 to 160 min. The chemigram is a reconstruction that shows the infrared response from 2800 to 2980 cm^{-1} as a function of time. (c) FTIR spectrum of species evolving from 30 to 160 min.

assigned as the active carbon stretching mode of the nanotubes. Infrared bands in the 1000 cm^{-1} to 1500 cm^{-1} region may arise from the bending modes and umbrella (rocking) modes of the methyl groups.

Thermal gravimetric analyses of degassed (80 °C) derivatized SWNTs were used to evaluate the extent of sidewall functionalization. Figures 4 and 5 show TGA loss of weight data for alkylated l-SWNTs and h-SWNTs, respectively. The calculated

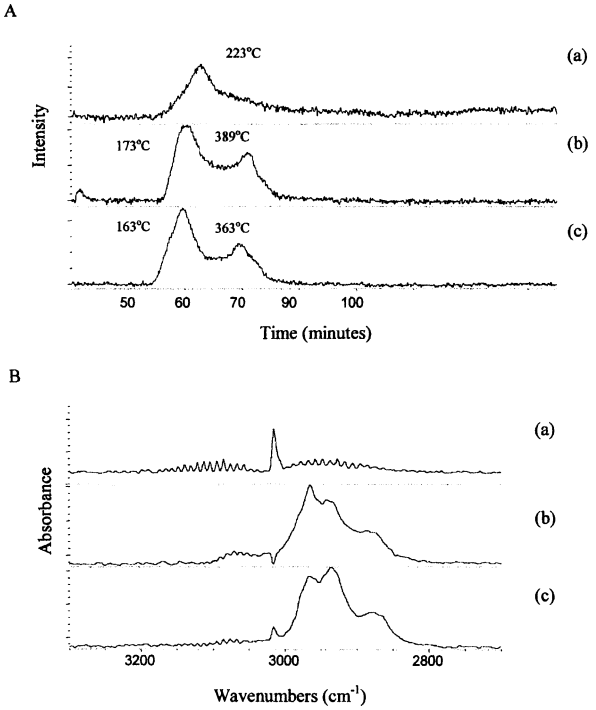

Figure 7. TGA-FTIR spectra of alkylated h-SWNTs. (A) Chemigram (intensity vs time) from TGA-FTIR spectra of alkylated h-SWNTs showing alkyl groups evolving from 30 to 160 min. The chemigram was recorded from 3000 to 3023 cm^{-1} for methyl h-SWNTs and from 2800 to 2980 cm^{-1} for *n*-butyl h-SWNTs and *n*-hexyl h-SWNTs (B) FTIR spectrum of species evolving from 30 to 80 min. Alkyl samples are labeled as: (a) methyl h-SWNTs; (b) *n*-butyl h-SWNTs; (c) *n*-hexyl h-SWNTs.

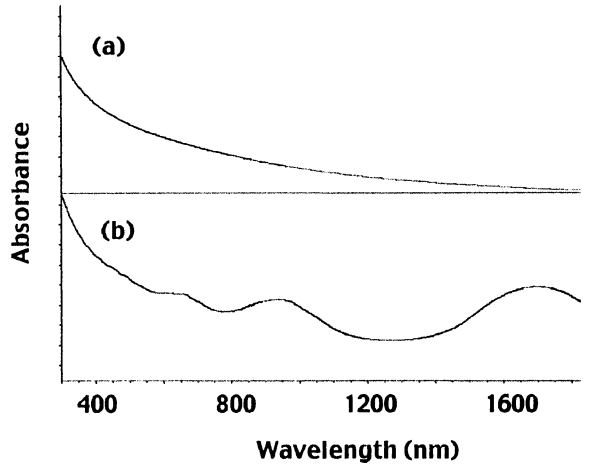

Figure 8. UV−vis-Nir spectra of l-SWNTs. (a) *n*-hexyl l-SWNTs; (b) *n*-hexyl l-SWNTs after heating in argon at 500 °C for 1 h.

carbon-to-alkyl group ratio (C/R) for methyl, *n*-butyl and *n*-hexyl SWNTs from TGA weight loss data are listed in Table 1 for both types of SWNTs. As expected, alkylation of HiPco SWNTs resulted in a higher degree of functionalization (thus more loss of weight), compared to that of laser-oven-grown SWNTs. This observation may be attributed to the smaller diameter of the HiPco SWNTs (about 1.0 nm) compared to the larger l-SWNTs (1.3 nm). The strain resulting from a higher degree of curvature accounts for the greater reactivity of the HiPco SWNTs.

The TGA-FTIR analysis of hexylated h-SWNTs are presented in Figures 6a−c. The derivative (weight loss with respect to time) plot (Figure 6a) shows two maxima which correspond to 163 °C and 363 °C. Chemigram (reconstruction that shows the

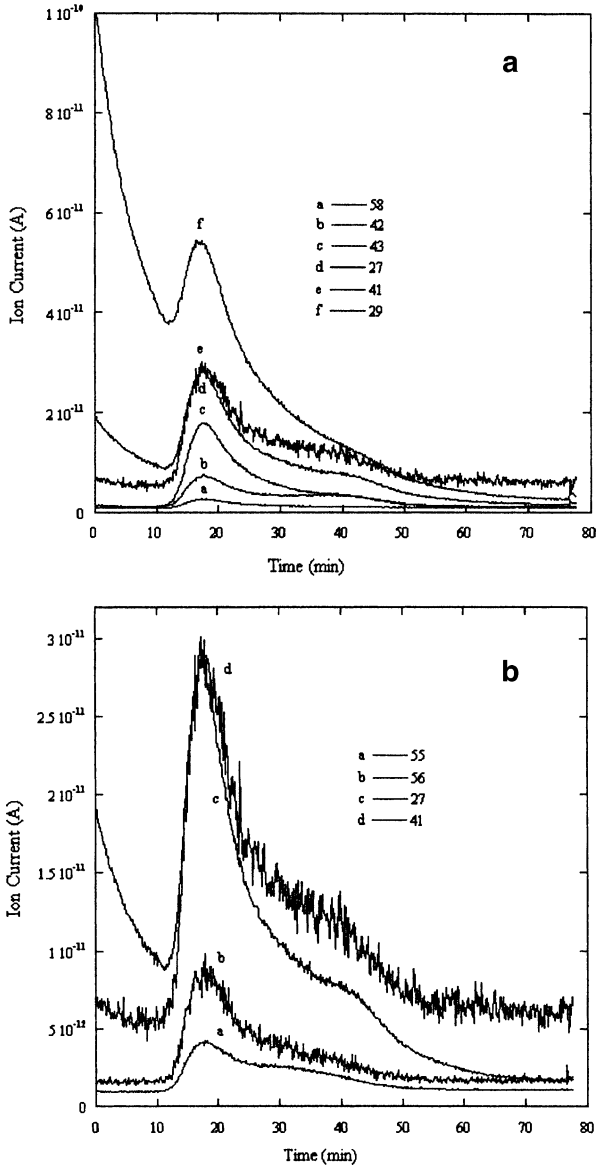

Figure 9. (a) Parent and fragment ions of *n*-butane from the TGA-MS analysis of *n*-butylated h-SWNTs. (b) Parent and fragment ions of 1-butene from the TGA-MS analysis of *n*-butylated h-SWNTs.

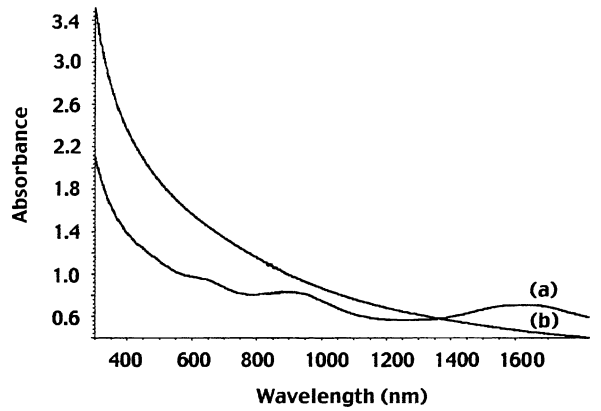

Figure 10. UV−vis−Nir spectra of alkylated l-SWNTs after reaction with (a) *tert*-butyllithium; (b) *n*-butyllithium.

infrared response over a specified wavenumber region as a function of time) of the C−H stretching region also shows two distinct peaks (Figure 6b). FTIR spectra of these time regimes

Table 2. Weight Gain and Carbon/Alkyl Group Ratio When l-SWNTs are Reacted with *n*-Hexyllithium at Room Temperature in Various Solvents[a]

solvent	weight gain (%)	C/R ratio
THF	24.3	21.6
ether	13.4	44.5
hexane	25.7	19.9
TMEDA	17.5	31.9

[a] TGA weight loss data were used to calculate values.

Table 3. Weight Gain at Room Temperature and −40 °C When l-SWNTs are Alkylated by *n*-Hexyllithium[a]

solvent	RT	−40 °C
THF	24.3	24.4
hexane	25.7	27.7

[a] TGA weight loss data were used to calculate values.

demonstrate the presence of hexyl groups (Figure 6c). The result with the alkylated h-SWNTs are presented in Figure 7.

The spectral signature of the pristine SWNTs can be regenerated when the alkylated SWNTs are heated in Ar at 500 °C, demonstrating that dealkylation occurs at this temperature (Figure 8). The mechanism of the dealkylation reaction was probed by TGA-MS analysis. The volatile products formed from *n*-butylated SWNTs were identified as 1-butene and *n*-butane. These results are presented in Figure 9a,b for 1-butene and *n*-butane, respectively. The formation of 1-butene suggests that the *n*-butyl groups detach from the SWNT as radicals which then disproportionate to form the two hydrocarbons. However, detachment of the hydrocarbon fragment from the SWNT via a β-elimination cannot be ruled out. This would leave hydrogen bound to the SWNT which could be abstracted by the *n*-butyl radical to form *n*-butane.

Steric effects were evaluated by comparing the relative reactivities of *n*-butyllithium and *tert*-butyllithium. Whereas the van Hove transition disappears for the products from the reaction using *n*-butyllithium, it is somewhat lower in relative intensity, yet observable, for the reaction with *tert*-butyllithium (Figure 10). As expected, the weight loss after heating in argon for *tert*-butyl SWNTs is less than *n*-butyl SWNTs, confirming that *tert*-butyllithium is less effective as an alkylating agent since both groups have the same molecular mass.

The effect of solvent on the alkylation reactions was also investigated. Fluorotubes are soluble in THF, but not in *n*-hexane or ether. Table 2 shows the weight gain when l-SWNTs were reacted with *n*-hexyllithium at room temperature in various solvents.

The effect of temperature is negligible when reactions are carried out in THF at room temperature and − 40 °C; however, a significant increase of alkyl attachment was observed when the alkylation reactions were carried out in *n*-hexane. A study using l-SWNTs showed that the yield may be optimized by lowering the reaction temperature in *n*-hexane solution (Table 3).

These results are consistent with a multistep process that is initiated by one-electron transfer from the alkyllithium reagent to the nanotube. Expulsion of fluoride from the resulting radical anion would lead to a radical site on the SWNT. Recombination of the alkyl radical with the SWNT would lead to the alkylated nanotube. Crowding of alkyl groups suggests that not every fluorine would be replaced by an alkyl group. Steric effects probably account for the observation that more extensive alkylation occurs when less sterically demanding methyllithium is used. Additional support for the electron-transfer process comes from the fact that phenyllithium which is known to react by a two-electron process does not react with fluorinated SWNTs.

Conclusion

We have demonstrated that alkyllithium reagents may be used to attach alkyl groups to the sidewalls of fluorinated nanotubes. Thermal gravimetric analysis combined with UV−vis−Nir spectroscopy provides a measure of the degree of functionalization. h-SWNTs exhibit a higher degree of alkylation than the l-SWNTs, indicating that smaller diameter tubes are more reactive to the chemical environment. The pristine nanotubes can be recovered after thermolysis demonstrating that dealkylation occurs at the higher temperature. TGA-MS analyses were used to identify *n*-butane and 1-butene as the products that are formed when *n*-butylated SWNTs are subjected to thermolysis. Chemical modification on the sidewall by alkylation leads to derivatives that are soluble in common organic solvents such as tetrahydrofuran and chloroform. Future studies will focus on cross-linking of SWNTs as a route to new materials that might be useful in the manufacture of nanotube fibers and composites.

Acknowledgment. We gratefully acknowledge the National Science Foundation, the Welch Foundation and the ATP for support of this work.

JA021167Q